

MARIOLA BUCZKOWSKA
GRZEGORZ DERFEL

Institute of Physics, Technical University of Lodz
Wólczańska 219, 90-924 Łódź, Poland. e-mail: mbuczko@p.lodz.pl

ROLE OF IONS MOBILITY IN FLEXOELECTRIC DEFORMATIONS OF CONDUCTIVE HOMEOTROPIC NEMATIC LAYERS

Numerical studies of d.c. electric field induced deformations of homeotropic layers of flexoelectric nematics containing ions are presented. It is shown that anomalous dependencies of threshold voltage for deformations on ion concentration, which were found in our previous papers, are due to difference between mobilities of cations μ^+ and anions μ^- . The influence of this difference on the deformations is analyzed. The set of equations describing the director orientation, the electric potential and the ion concentrations as functions of the coordinate normal to the layer, is solved. The calculations are performed for four types of nematic materials characterized by both signs of dielectric anisotropy and of the sum of flexoelectric coefficients. Finite surface anchoring strength is assumed. It is shown that the anomalies concerning the threshold vanish if μ^+ becomes equal to μ^- . The results are explained by means of qualitative analysis of the electric field distributions.

Keywords: nematics, flexoelectricity, ion mobility.

1. INTRODUCTION

Operation of liquid crystal devices of any type is based on electric field induced deformations of liquid crystal layers confined between transparent electrodes. External electric field influences the director distribution and changes the optical properties of the layer. The most common electro-optic effects occur as a result of the torque acting in the bulk of the layer due to dielectric anisotropy $\Delta\epsilon$. Deformation of dielectric nature is a quadratic effect and

therefore does not depend on the sign of the voltage. There is also another kind of interaction between the bias electric field and the nematic liquid crystal, namely the flexoelectric effect, which offers applications in displays.

Nematic materials usually possess flexoelectric properties due to asymmetric shape and dipolar nature of mesogenic molecules [1]. Flexoelectricity manifests itself by arising of electric polarization whenever the director distribution contains splay or bend (which is called the direct flexoelectric effect), as well as by deformation resulting from the interaction between the flexoelectric polarization and the applied electric field (which is known as the converse flexoelectric effect). In both cases, the coupling of the field with the flexoelectric polarization is linear. The field effects depend therefore on the sign of the bias voltage which offers new possibilities of controlling the director reorientation. The flexoelectric properties are described by two flexoelectric coefficients e_{11} and e_{33} which determine the relationship between the deformation of the nematic and the electric polarization $\mathbf{P} = e_{11} \mathbf{n}(\nabla \cdot \mathbf{n}) - e_{33} \mathbf{n} \times (\nabla \times \mathbf{n})$. The role of flexoelectricity in the behaviour of the liquid crystal systems is investigated in various aspects for nearly forty years. Numerous works were devoted to the electric field induced deformations of flexoelectric nematic layers (e.g. [2-9]). These phenomena still attract attention of liquid crystal researchers due to their potential electro-optical applications. Flexoelectricity plays a crucial role in switching between stable states in the Zenithal Bistable Device [10,11].

The occurrence and form of the elastic deformations depend on the relationship between the magnitudes and signs of flexoelectric torques as well as on the magnitude and sign of the dielectric torque. The flexoelectric contribution to the deformations is due to the torques acting in the bulk whenever the director distribution is non-homogeneous and/or there exists an electric field gradient. In the latter case, the so called gradient flexoeffect occurs [2,3,9]. Another contribution to the deformations is given by the flexoelectric torques acting on the director adjacent to the boundary surfaces. Simultaneously, the deformations are affected by dielectric torque acting in the bulk which is proportional to the square of the electric field strength.

Let us consider one-dimensional deformations of homeotropic flexoelectric nematic layers subjected to the electric field applied normal to the layers planes. They depend on the signs and magnitudes of dielectric anisotropy and of the sum $e = e_{11} + e_{33}$ of flexoelectric coefficients. In the case of perfectly insulating nematic, the deformations of the homeotropic layer are possible if the inequality

$$(e_{11} + e_{33})^2 > k_{33} \epsilon_0 \Delta \mathcal{E} \quad (1)$$

is satisfied [4]. They arise above a threshold voltage U_f which is given by the formula

$$\coth\left(\pi \frac{U_f}{U_c}\right) = \frac{Wd}{2\pi k_{33}} \frac{U_c}{U_f} \left\{ \left(\frac{\pi k_{33} U_f}{Wd U_c} \right)^2 \left[\left(\frac{U_c (e_{11} + e_{33})}{\pi k_{33}} \right)^2 - 1 \right] - 1 \right\} \quad (2a)$$

if $\Delta\epsilon > 0$, and by

$$\cot\left(\pi \frac{U_f}{U_c}\right) = \frac{Wd}{2\pi k_{33}} \frac{U_c}{U_f} \left\{ \left(\frac{\pi k_{33} U_f}{Wd U_c} \right)^2 \left[\left(\frac{U_c (e_{11} + e_{33})}{\pi k_{33}} \right)^2 + 1 \right] - 1 \right\} \quad (2b)$$

if $\Delta\epsilon < 0$, where $U_c = \pi \sqrt{k_{33}/(\epsilon_0 |\Delta\epsilon|)}$, W is the anchoring strength, k_{33} is the bend elastic constant and d is the thickness of the layer [4].

The space charge of ions, which are always present in liquid crystal, plays a crucial role in the deformations since it influences the electric field distribution. The spatial distribution of ions is in turn dependent on the electrical properties of the nematic, in particular on the ion mobilities and on the properties of the electrodes. These properties govern the ionic charges accumulation at the electrodes and give rise to a non-homogeneity of the electric field. The flexoelectric torque due to the electric field gradient influence the deformations, in particular the value of the threshold voltage. The deformations induced by the non-homogeneous field resulting from the accumulation of ions has been experimentally observed and theoretically described by Derzhanski and co-workers already at an early stage of investigations of flexoelectricity [2,3,9].

In our previous papers [12-14], we presented numerical calculations concerning the influence of ionic transport on deformations of homeotropic nematic layers possessing flexoelectric properties. Four types of nematic materials characterized by both signs of $\Delta\epsilon$ and by both signs of e were taken into account. Several peculiar effects manifested by various dependencies of threshold voltage on the ion concentration were predicted. These effects were most representative for moderate ion concentrations ($\sim 10^{19} \text{ m}^{-3}$) and for blocking electrode contacts. (If the ion content was low or if the electrodes were well conducting, such peculiarities were absent and the layer behaviour was qualitatively similar to that of insulating nematic.) They can be briefly described as follows:

- (i) in the case of negative dielectric anisotropy and negative sum of the flexoelectric coefficients, the threshold voltage for deformations reached exceptionally high values which exceeded the theoretical U_f characteristic for the perfectly insulating nematic. [12]

- (ii) in the case of negative dielectric anisotropy and positive sum of the flexoelectric coefficients, the threshold voltage was much lower than U_f [13]
- (iii) in the case of positive dielectric anisotropy and negative sum of the flexoelectric coefficients, the threshold voltage was also lower than U_f [14]
- (iv) in the case of positive dielectric anisotropy and positive sum of the flexoelectric coefficients, the deformations occurred in two voltage regimes i.e. it appeared, disappeared and reappeared again with the increasing voltage. The threshold voltage exceeding the U_f value was also found. [14]

These effects were caused by the non-uniformity of electric fields existing in the layer. The non-uniform field arose due to the ionic space charge present in the layer and was influenced by the quantities which decided on the ion transport, namely the ion concentrations, their mobilities and electrode properties.

Some preliminary results presented in [13] suggest that these effects are due to large difference between mobilities μ^+ and μ^- of cations and anions, which was adopted according to the opinion that the cations are much less mobile than the anions [15,16]. Therefore it seems to be important to study a role of this difference. For this purpose, we performed numerical calculations for several μ^+/μ^- ratios and for all the four types of nematic materials studied earlier. In this paper, we present results of such studies. We restricted our attention to the case of strongly blocking and poorly conducting electrodes.

The results show that the peculiarities concerning the threshold become less pronounced if μ^+/μ^- ratio tends to 1, assuming that $\mu^- = \text{const} = 10^{-9} \text{ m}^2\text{V}^{-1}\text{s}^{-1}$. In particular, the lower of the two voltage regimes, observed when $\Delta\epsilon > 0$ and $e > 0$, disappears. In the limiting case of $\mu^+/\mu^- = 1$, the threshold values are neither enhanced with respect to the value U_f , as it was found for $\Delta\epsilon < 0$ and $e < 0$, nor lowered drastically as in the case of $\Delta\epsilon < 0$ and $e > 0$. Disappearance of the peculiarities mentioned above is due to changes of the space charge distributions which are caused by changes of the ion mobilities ratio. For the same reason, the form of deformation (determined by the dependence of the director orientation angle on the coordinate) is also affected by the μ^+/μ^- ratio. The torques which decide on the director configurations depend on the electric field distributions, which in turn depend on the ionic space charge.

In the next section, the parameters of the system under consideration are given and the basic equations are gathered. In section 3, the results of calculations are presented; these are discussed in section 4. Conclusions are given briefly in section 5.

2. GEOMETRY, PARAMETERS AND METHOD

The simulations concerned the nematic liquid crystals confined between two infinite plates which played the role of electrodes and were parallel to the x,y -plane of the Cartesian coordinate system and positioned at $z = \pm d/2$. A voltage U was applied between them. The lower electrode ($z = -d/2$) was earthed. Homeotropic alignment was assumed. The director \mathbf{n} was parallel to the x,z -plane; its orientation was described by the angle $\theta(z)$, measured between \mathbf{n} and the z axis. The material and layer parameters were similar as in our previous papers [12-14] and are mentioned below. The thickness of the layer was $d = 20 \mu\text{m}$. The calculations were performed for four types of nematic materials characterized by both signs of the dielectric anisotropy $\Delta\epsilon$ and by both signs of the sum of flexoelectric coefficients e : $\Delta\epsilon = -0.7$ and $e = -40 \text{ pCm}^{-1}$; $\Delta\epsilon = -0.7$ and $e = 40 \text{ pCm}^{-1}$; $\Delta\epsilon = 2$ and $e = -40 \text{ pCm}^{-1}$; $\Delta\epsilon = 2$ and $e = 40 \text{ pCm}^{-1}$. The dielectric tensor component normal to the director was $\epsilon_{\perp} = 5.4$. The anchoring strength W was identical on both surfaces and was equal to 10^{-5} Jm^{-2} in the case of $\Delta\epsilon = -0.7$ and $2 \times 10^{-5} \text{ Jm}^{-2}$ when $\Delta\epsilon = 2$. The model substances were characterized by the elastic constants $k_{11} = 6.2 \times 10^{-12} \text{ N}$ and $k_{33} = 8.6 \times 10^{-12} \text{ N}$.

The transport of the ions under the action of an electric field was characterized by their mobility and diffusion coefficients. The order of magnitude of mobilities corresponded to typical values measured for various liquid crystals [17,18]. We adopted constant mobility of anions, $\mu_{\perp}^{-} = 1 \times 10^{-9}$, whereas the mobilities of cations were varied and equal to $\mu_{\perp}^{+} = 1 \times 10^{-10}$, $\mu_{\perp}^{+} = 3 \times 10^{-10}$ and $\mu_{\perp}^{+} = 1 \times 10^{-9} \text{ m}^2 \text{V}^{-1} \text{s}^{-1}$ respectively, to give three ratios of μ^{+}/μ^{-} : 0.1, 0.3, and 1 in order to demonstrate the role of this ratio in the flexoelectric deformations. Typical anisotropy of mobility i.e. $\mu_{\parallel}^{\pm}/\mu_{\perp}^{\pm} = 1.5$ was assumed. The Einstein relation was assumed for the diffusion constants: $D_{\parallel,\perp}^{\pm} = (k_B T/q) \mu_{\parallel,\perp}^{\pm}$, where q denotes the absolute value of the ionic charge, k_B is the Boltzmann constant and T is the absolute temperature.

The weak electrolyte model [19] was adopted for the description of the electrical phenomena in the layer. The ion concentration was determined by the generation constant $\beta = \beta_0 \left(1 + \frac{q^3}{8\pi\epsilon_0 \bar{\epsilon} k_B^2 T^2} E \right)$ where $\bar{\epsilon} = (2\epsilon_{\perp} + \epsilon_{\parallel})/3$ (the parameter β_0 was varied between $10^{18} \text{ m}^{-3} \text{s}^{-1}$ and $10^{24} \text{ m}^{-3} \text{s}^{-1}$ in order to control the ion concentration), and by the recombination constant $\alpha = \frac{2q\bar{\mu}}{\epsilon_0 \bar{\epsilon}}$ where

$\bar{\mu} = [(2\mu_{\perp}^+ + \mu_{\parallel}^+)/3 + (2\mu_{\perp}^- + \mu_{\parallel}^-)/3]/2$ [20]. The resulting average ion concentration N_{av} , defined as

$$N_{av} = \frac{1}{2} \left\{ \int_{-1/2}^{1/2} [N^+(\zeta) + N^-(\zeta)] d\zeta \right\}, \quad (3)$$

where $N^{\pm}(\zeta)$ denote the concentrations of ions of corresponding sign and $\zeta = z/d$ is the reduced coordinate, ranged from 10^{17} to $5 \times 10^{20} \text{ m}^{-3}$.

The electrode processes were described in terms of our model which has been presented in detail in [12,13]. According to this model, the flux of ions of given sign which approach a chosen electrode (or move away from it) is equal to the net change in the number of ions resulting from the generation and neutralisation processes at the electrode per unit area and per unit time. The speed of neutralisation of the ions, n_r^{\pm} , is proportional to their concentration: $n_r^{\pm} = K_r^{\pm} N^{\pm}$ and the speed of generation, n_g^{\pm} , is proportional to the concentration N_d of the neutral dissociable molecules: $n_g^{\pm} = K_g^{\pm} N_d$, where K_r^{\pm} and K_g^{\pm} are suitable constants of proportionality and $N_0 = \sqrt{\beta_0/\alpha}$. In general, K_r^{\pm} and K_g^{\pm} can be different for each electrode process. For simplicity however, the calculations were performed using a common value of K_r for all neutralization processes as well as a common value of $K_g = K_r N_0 / N_d$ for all generation processes at the electrodes.

The rates of generation and neutralisation of the ions at the electrodes can be interpreted in terms of activation energies φ of corresponding electrochemical reactions due to energy barriers arising between the liquid crystal and electrodes. For example, the rate of neutralization of a negative ion occurring by the transfer of an electron from the ion to the electrode is equal to $K_r = k_r \exp(-\varphi/k_B T)$, where k_r is a constant. A similar formula can be used for the generation constant of positive ions occurring by the transfer of an electron from a neutral molecule to the electrode. (In general, the energy barriers φ can be of different height for every electrode process.) The energy barrier is affected by the electric field existing at the electrode, i.e. increased or decreased by $\Delta\varphi = |E|qL$, where L is the thickness of the subelectrode region, of the order of several molecular lengths. In our calculations $L = 10 \text{ nm}$ was assumed.

The peculiar effects mentioned in section 1 were predicted for the strongly blocking and poorly conducting electrode contacts. Therefore our present

calculations were carried out with two values of K_r , 10^{-7} and 10^{-5} m s^{-1} , corresponding to these cases.

The problem is considered to be one-dimensional. The system is determined by a set of ten equations [12]. The bulk properties of the layer are described by a torque equation

$$\begin{aligned} & \frac{1}{2}(k_b - 1)\sin 2\theta \left(\frac{d\theta}{d\zeta} \right)^2 - (\sin^2 \theta + k_b \cos^2 \theta) \frac{d^2 \theta}{d\zeta^2} + \frac{1}{2} \frac{\varepsilon_0 \Delta \varepsilon}{k_{11}} \sin 2\theta \left(\frac{dV}{d\zeta} \right)^2 \\ & + \frac{1}{2} \frac{e_{11} + e_{33}}{k_{11}} \sin 2\theta \left(\frac{d^2 V}{d\zeta^2} \right) = 0 \end{aligned} \quad (4)$$

where $k_b = k_{33}/k_{11}$, an electrostatic equation

$$\begin{aligned} & \rho(\zeta) d^2 + \varepsilon_0 (\varepsilon_{\perp} + \Delta \varepsilon \cos^2 \theta) \frac{d^2 V}{d\zeta^2} - \varepsilon_0 \Delta \varepsilon \sin 2\theta \frac{dV}{d\zeta} \frac{d\theta}{d\zeta} + (e_{11} + e_{33}) \cos 2\theta \left(\frac{d\theta}{d\zeta} \right)^2 \\ & + \frac{1}{2} (e_{11} + e_{33}) \sin 2\theta \frac{d^2 \theta}{d\zeta^2} = 0 \end{aligned} \quad (5)$$

where $\rho(\zeta) = q[N^+(\zeta) - N^-(\zeta)]$ is the space charge density, and two equations of continuity of anions and cations fluxes in the bulk

$$d(\beta - \alpha N^+ N^-) = \frac{d}{d\zeta} \left[\mp \frac{1}{d} \left(\mu_{zz}^{\pm} N^{\pm} \frac{dV}{d\zeta} \pm D_{zz}^{\pm} \frac{dN^{\pm}}{d\zeta} \right) \right] \quad (6)$$

where $\mu_{zz}^{\pm} = \mu_{\perp}^{\pm} + \Delta \mu^{\pm} \cos^2 \theta$, $D_{zz}^{\pm} = D_{\perp}^{\pm} + \Delta D^{\pm} \cos^2 \theta$, $\Delta \mu^{\pm} = \mu_{\parallel}^{\pm} - \mu_{\perp}^{\pm}$ and $\Delta D^{\pm} = D_{\parallel}^{\pm} - D_{\perp}^{\pm}$.

The boundary conditions for the orientation angle are given by two torque equations for the boundaries

$$\begin{aligned} & \pm \left[\frac{1}{2} \frac{e_{11} + e_{33}}{k_{11}} \sin 2\theta(\pm 1/2) \frac{dV}{d\zeta} \Big|_{\pm 1/2} - (\sin^2 \theta(\pm 1/2) + k_b \cos^2 \theta(\pm 1/2)) \frac{d\theta}{d\zeta} \Big|_{\pm 1/2} \right] \\ & - \frac{1}{2} \gamma \sin 2\theta(\pm 1/2) = 0 \end{aligned} \quad (7)$$

for $\zeta = \pm 1/2$ respectively, where $\gamma = Wd/k_{11}$. Boundary conditions for the electrostatic potential, $V(\zeta)$, are $V(-1/2) = 0$ and $V(1/2) = U$. The boundary conditions for ion transfer across the electrode contacts are determined by four equations:

$$\mp \mu_{zz}^{\pm} N^{\pm} \frac{dV}{d\zeta} - D^{\pm} \frac{dN^{\pm}}{d\zeta} = [-N^{\pm} K_r \exp(\pm \Delta\phi/k_B T) + N_0 K_r \exp(\mp \Delta\phi/k_B T)] d \quad (8)$$

for $\zeta = -1/2$ and

$$\mp \mu_{zz}^{\pm} N^{\pm} \frac{dV}{d\zeta} - D^{\pm} \frac{dN^{\pm}}{d\zeta} = -[-N^{\pm} K_r \exp(\mp \Delta\phi/k_B T) + N_0 K_r \exp(\pm \Delta\phi/k_B T)] d \quad (9)$$

for $\zeta = 1/2$. The left hand sides of equations (8) and (9) represent the fluxes of the ions at the electrodes. The first terms on the right hand sides denote the numbers of ions which are neutralised; the second terms denote the numbers of ions generated at the electrodes in the course of accepting or donating electrons by neutral molecules.

The numerical solutions allowed us to plot the threshold voltage U_T (with an accuracy of 0.01 V) as a function of average ion concentrations N_{av} and the electric field strength distributions $|E|(\zeta)$.

3. RESULTS

The threshold voltages obtained from the calculations are presented in figures 1-4. Thick lines denote the poorly conducting electrode contacts and thin lines concern the strongly blocking electrodes characterized by $K_r = 10^{-5} \text{ ms}^{-1}$ and $K_r = 10^{-7} \text{ ms}^{-1}$ respectively.

3.1. Threshold voltage

All the deformations have threshold character. The threshold voltage U_T depends on the average ion concentrations, on the properties of the electrodes as well as on the ions mobility. The peculiarities described in our previous papers [12-14] occurred mainly in the range of the moderate ion concentrations. The threshold was then enhanced or lowered or the deformations appeared, disappeared and reappeared again with the increasing voltage, i.e. two voltage regimes existed in which the layer was distorted. All those effects took place only if the electrodes had strongly blocking or poorly conducting character. In this paper, we show that peculiarities in question are not so expressive and even disappear when the ratio of mobilities μ^+/μ^- of ions of both signs increases and tends to 1. In order to show in detail the changes of the form of deformations caused by variation of mobilities ratio, we performed the calculations for $\mu^+/\mu^- = 0.1, 0.3$ and 1. In the case of negative dielectric anisotropy and negative sum of the flexoelectric coefficients, additional ratio equal to 0.5 was used. Figures 1, 2, 3 and 4 illustrate the dependence of the threshold voltage U_T on the

average ion concentration N_{av} . The data concern four cases which differ in signs of the dielectric anisotropy and of the sum of flexoelectric coefficients. Please note that in the case of equal mobilities of anions and cations, the sign of the sum of flexoelectric coefficients is not essential.

3.1.1. $\Delta\epsilon < 0$ and $e_{11} + e_{33} < 0$. In figure 1, the decay of the threshold enhancement is shown. For example, the threshold reaches c. 6.25 V if the ratio of the mobilities is 0.1 (curves 1 and 5). As the ratio increases, the threshold is lowered gradually. This effect becomes evident if $\mu^+/\mu^- \geq 0.5$ (curves 3 and 7). In the limiting case of $\mu^+/\mu^- = 1$, the threshold achieves a low value, about 3.3 - 3.5 V (curves 4 and 8), which is close to the value U_f found for an insulating nematic.

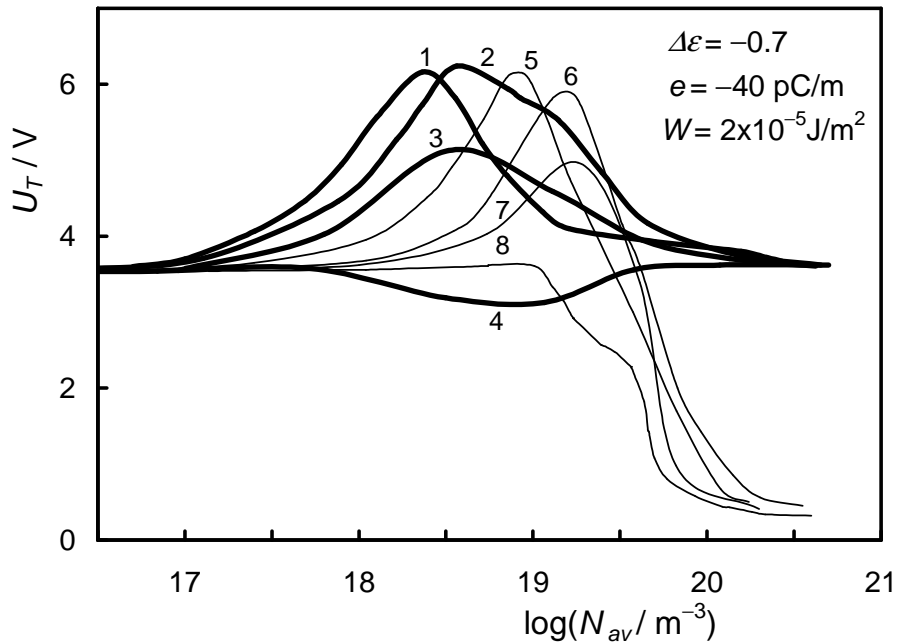


Fig. 1. Threshold voltage U_T as a function of average ion concentration N_{av} , for two values of Kr . $\Delta\epsilon = -0.7$, $e = -40$ pC/m, $W = 2 \times 10^{-5}$ J/m². Thick lines: $Kr = 10^{-5}$ ms⁻¹, thin lines: $Kr = 10^{-7}$ ms⁻¹. Mobility ratios μ^+/μ^- are as follows: lines 1 and 5: $\mu^+/\mu^- = 0.1$; lines 2 and 6: $\mu^+/\mu^- = 0.3$; lines 3 and 7: $\mu^+/\mu^- = 0.5$; lines 4 and 8: $\mu^+/\mu^- = 1$

3.1.2. $\Delta\epsilon < 0$ and $e_{11} + e_{33} > 0$. Figure 2 shows how the reduction of threshold decays during the increase of the mobilities ratio. The threshold value grows

from c. 1.3 V observed for $\mu^+/\mu^- = 0.1$ (curves 1 and 4) to about 3.3 V for $\mu^+/\mu^- = 1$ (curves 3 and 6).

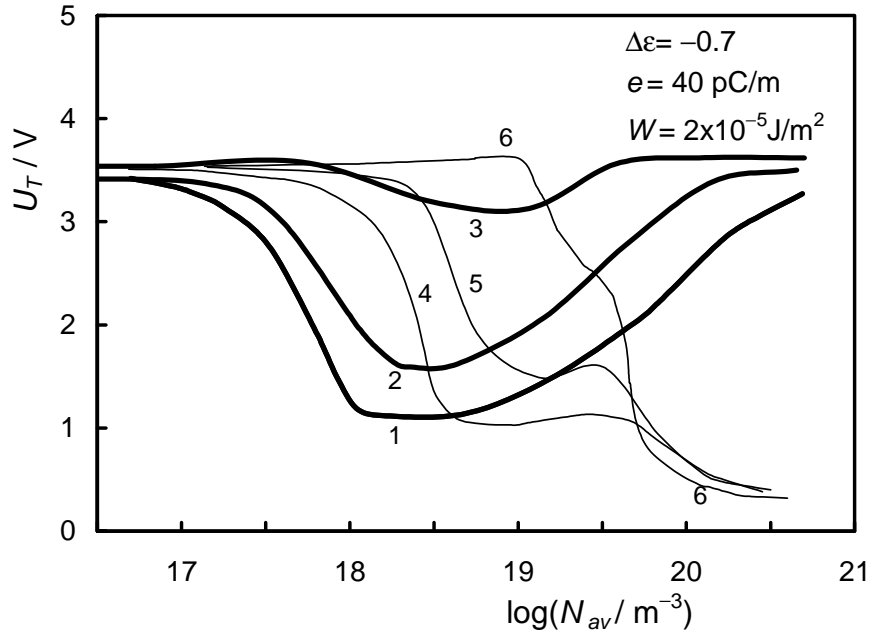


Fig. 2. Threshold voltage U_T as a function of average ion concentration N_{av} , for two values of Kr . $\Delta\epsilon = -0.7$, $e = 40$ pC/m, $W = 2 \times 10^{-5}$ J/m². Thick lines: $Kr = 10^{-5}$ ms⁻¹, thin lines: $Kr = 10^{-7}$ ms⁻¹. Mobility ratios μ^+/μ^- are as follows: lines 1 and 4: $\mu^+/\mu^- = 0.1$; lines 2 and 5: $\mu^+/\mu^- = 0.3$; lines 3 and 6: $\mu^+/\mu^- = 1$

3.1.3. $\Delta\epsilon > 0$ and $e_{11} + e_{33} < 0$. When the mobility ratio is low, the threshold voltage is significantly lower than U_f (figure 3, curves 1 and 4). With increasing value of μ^+/μ^- , the threshold becomes greater. This effect is less pronounced for $Kr = 10^{-7}$ ms⁻¹. In the case of $Kr = 10^{-5}$ ms⁻¹, the $U_T(N_{av})$ dependence becomes the weaker, the larger is μ^+/μ^- , (curves 2 and 3).

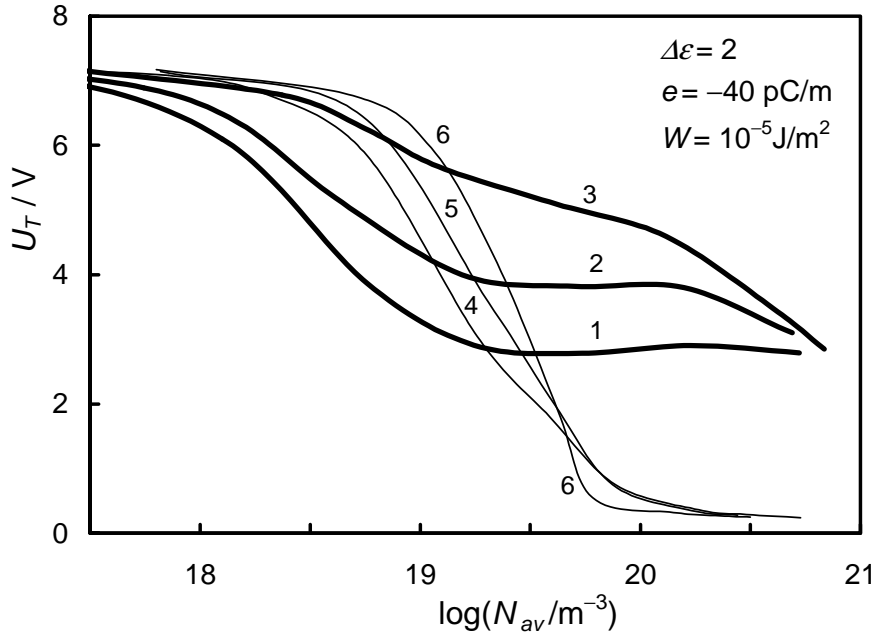


Fig. 3. Threshold voltage U_T as a function of average ion concentration N_{av} , for two values of K_r . $\Delta\epsilon = 2$, $e = -40$ pC/m, $W = 10^{-5}$ J/m². Thick lines: $K_r = 10^{-5}$ ms⁻¹, thin lines: $K_r = 10^{-7}$ ms⁻¹. Mobility ratios μ^+/μ^- are as follows: lines 1 and 4: $\mu^+/\mu^- = 0.1$; lines 2 and 5: $\mu^+/\mu^- = 0.3$; lines 3 and 6: $\mu^+/\mu^- = 1$

3.1.4. $\Delta\epsilon > 0$ and $e_{11} + e_{33} > 0$. In the case of $\mu^+/\mu^- = 0.1$, two voltage regimes exist, in which the deformations occur (figure 4, curves 1 and 4). Additionally, for $K_r = 10^{-5}$ ms⁻¹, the upper threshold voltage reaches rather high value of c. 12 V, which is much higher than U_f (curve 1) whereas it remains close to U_f if $K_r = 10^{-7}$ ms⁻¹.

The lower voltage regime disappears when the mobilities ratio increases. This effect is illustrated in figure 5, where the optical phase difference $\Delta\Phi$ (used as an indication of a deformation arising under the action of bias voltage) is plotted as a function of cations mobility under the assumption that $\mu^- = 10^{-9}$ m²V⁻¹s⁻¹. It is evident that the deformation decays for quite low mobilities ratio. For example, when $K_r = 10^{-5}$ ms⁻¹, $N_{av} = 3.9 \times 10^{19}$ m⁻³ and $U = 3.5$ V, the limiting value of μ^+/μ^- is 0.115 (curve 2).

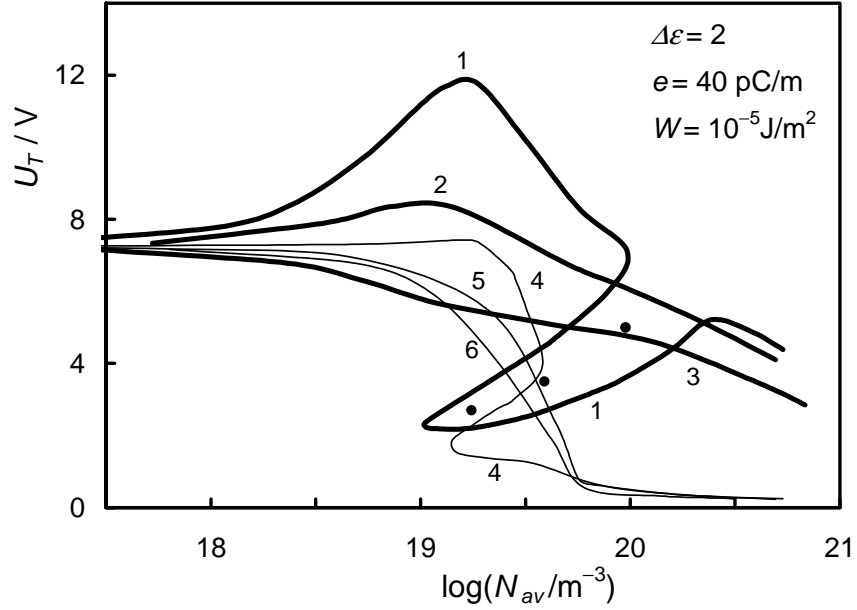


Fig. 4. Threshold voltage U_T as a function of average ion concentration N_{av} , for two values of Kr . $\Delta\epsilon = 2$, $e = 40$ pC/m, $W = 10^{-5}$ J/m². Thick lines: $Kr = 10^{-5}$ ms⁻¹, thin lines: $Kr = 10^{-7}$ ms⁻¹. Mobility ratios μ^+/μ^- are as follows: lines 1 and 4: $\mu^+/\mu^- = 0.1$; lines 2 and 5: $\mu^+/\mu^- = 0.3$; lines 3 and 6: $\mu^+/\mu^- = 1$. Full circles correspond to three curves presented in fig. 5

When $\mu^+/\mu^- = 0.3$, the deformation occurs in only one voltage range. The threshold voltage decreases monotonically with N_{av} (figure 4, curves 2 and 5). The same concerns the case of equal mobilities (curves 3 and 6).

4. DISCUSSION

In this paper, we consider the flexoelectric deformations of homeotropic nematic liquid crystal layer subjected to a d.c. electric field, in which the ratio of mobilities of cations and anions plays a crucial role. The results presented above were obtained for a homeotropic layers containing nematic materials with both signs of the dielectric anisotropy $\Delta\epsilon$ and both signs of the sum of flexoelectric coefficients $e_{11} + e_{33}$. Three ratios of μ^+/μ^- , 0.1, 0.3 and 1, were considered.

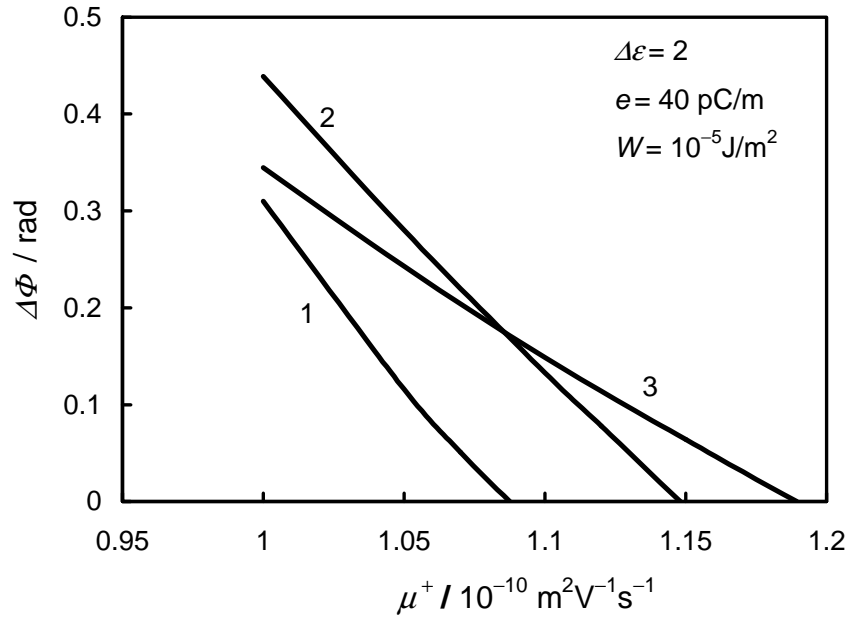


Fig. 5. Optical phase difference $\Delta\Phi$ as a function of cations mobility μ^+ . $\Delta\epsilon = 2$, $e = 40$ pC/m, $W = 10^{-5}$ J/m². $Kr = 10^{-5}$ ms⁻¹; $\mu^- = 10^{-9}$ m²V⁻¹s⁻¹; refractive indices: $n_o = 1.520$; $n_e = 1.672$; wavelength: $\lambda = 632.8$ nm. Voltages are as follows: line 1: $U = 5$ V, line 2: $U = 3.5$ V, line 3: $U = 2.7$ V

In the following, qualitative explanation as to why the deformation occurs, or why it does not occur is proposed by of analysis of the electric field strength distributions within the layer which allows the estimate of contributions of the various torques. Such an analysis of the torques is possible only *a posteriori*. The only predictive way is the numerical solution of the set of ten equations given in section 2.

For equal mobilities of ions of both signs, an approximate symmetry of electric field strength distributions was observed. In the rest of the cases, when $\mu^+/\mu^- < 1$, the electric field strength distributions were asymmetric. This effect resulted from the asymmetric ion distributions which had their origin in the difference between mobilities of positive and negative ions. The electric field strength distributions are shown in figures 6-9, for several selected cases characterized by both signs of $\Delta\epsilon$ and e . The relationships $|E|(\zeta)$ have similar forms but their interpretation is qualitatively different due to different torques acting on director in the bulk as well as at the boundaries. The deformations are

induced by torques of dielectric and flexoelectric nature. The dielectric torque is destabilizing if $\Delta\epsilon < 0$ and stabilizing in the opposite case. The flexoelectric torques depend on the sign of the sum of flexoelectric coefficients. Their action is illustrated in fig. 10 for the case of positive e . In the case of negative e , the signs of the torques are opposite.

Two extreme mobility ratios $\mu^+/\mu^- = 0.1$ (thin lines) and $\mu^+/\mu^- = 1$ (thick lines) are taken into account. The data concern the calculations performed for $K_r = 10^{-5} \text{ ms}^{-1}$. The average ion concentrations N_{av} were taken from the moderate range. They were chosen separately for each case in order to illustrate the most representative effects.

4.1. Reduction of threshold

4.1.1. $\Delta\epsilon < 0$ and $e_{11} + e_{33} > 0$. In figure 6, the electric field distributions calculated for $U = 1.15 \text{ V}$ are shown. This voltage value was chosen since it is equal to the threshold, U_T , at which the deformation starts for the case of unequal mobilities of ions, $\mu^+/\mu^- = 0.1$, while for the case of equal mobilities the layer remains undeformed at the same voltage. In both cases, we observe electric field gradient in the bulk. However, for unequal mobilities, the distribution of electric field is asymmetric and the electric field gradient dominates in the left half of the layer. This gradient gives rise to the destabilizing flexoelectric torque which initializes the deformations already at a threshold U_T reduced below U_f . On the contrary, for equal mobilities of ions, the gradients due to symmetric electric field distribution have opposite signs in the two halves of the layer. The destabilizing and stabilizing actions of the corresponding torques are partially compensated and the layer remains undeformed. Some higher voltage is required to induce deformation, which means that the threshold increases. Therefore in the case of $\mu^+ = \mu^-$ the reduction of U_T is absent.

4.1.2. $\Delta\epsilon > 0$ and $e_{11} + e_{33} < 0$. In this case, we also observe reduction of the threshold if $\mu^+ < \mu^-$. In figure 7, the electric field strength distributions for $U = 2.91 \text{ V}$ are shown. This value corresponds to U_T for $\mu^+/\mu^- = 0.1$, while the same voltage is not sufficient for deformation of the layer when the mobilities of cations and anions are equal. Since the deformation is limited to the vicinity of $\zeta = -1/2$, the destabilizing bulk flexoelectric torque due to the field gradient seems to be inessential, being overcome by the stabilizing action of the dielectric torque. The relation $\mu^+ < \mu^-$ causes an asymmetry of the electric field distribution. The deformation is induced by the surface field $|E(-1/2)|$ which takes very large value exceeding $|E(+1/2)|$. As a consequence, if $\mu^+/\mu^- = 0.1$, the

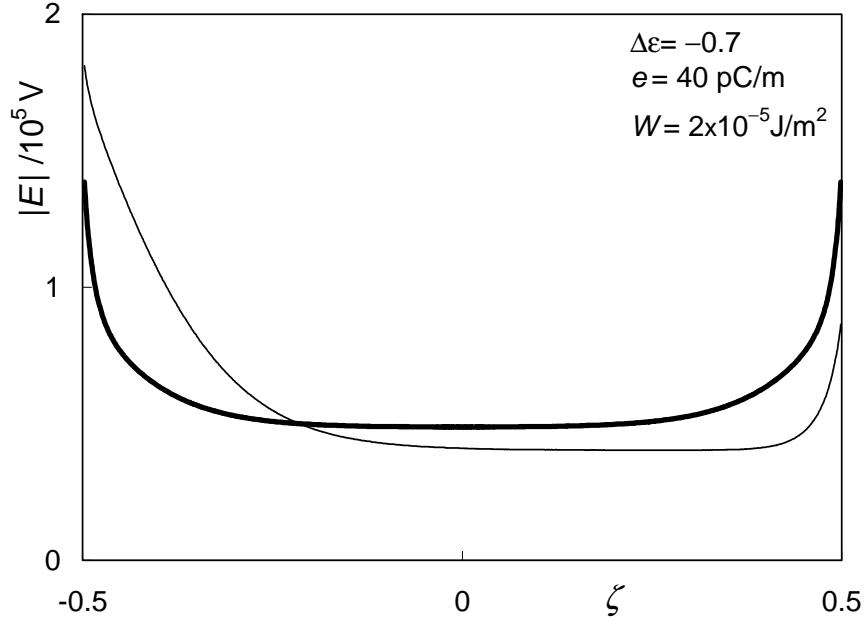


Fig. 6. Electric field strength $|E|$ as a function of the reduced coordinate ζ for $U = 1.15$ V, $Kr = 10^{-5}$ ms $^{-1}$ and $Nav = 5 \times 10^{18}$ m $^{-3}$. $\Delta\epsilon = -0.7$, $e = 40$ pC/m, $W = 2 \times 10^{-5}$ J/m 2 . Thick line: $\mu^+/\mu^- = 1$; thin line: $\mu^+/\mu^- = 0.1$

destabilizing surface flexoelectric torque at $\zeta = -1/2$ becomes sufficient for deformation at U_T much lower than U_f value. When $\mu^+ = \mu^-$, the asymmetry of the electric field distribution vanishes and the electric field value at $\zeta = -1/2$ is lower than in the case of $\mu^+/\mu^- = 0.1$, and is not sufficient to induce the deformation. In this case, some higher voltage is required for deformation of the layer *i.e.* the threshold reduction is much less pronounced.

4.2. Enhancement of threshold

4.2.1. $\Delta\epsilon < 0$ and $e_{11} + e_{33} < 0$. Figure 8 shows the electric field distribution calculated for $U = 3.19$ V. This voltage value is equal to the threshold at which the deformation arises when $\mu^+ = \mu^-$. On the contrary, for the same voltage the deformation does not occur if $\mu^+/\mu^- = 0.1$. This effect has the following reason.

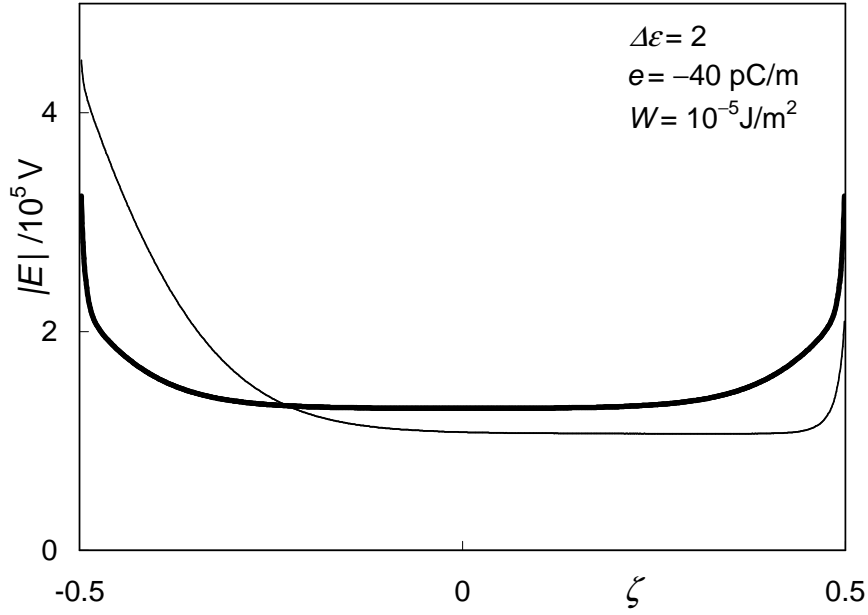


Fig. 7. Electric field strength $|E|$ as a function of the reduced coordinate ζ for $U = 2.91$ V, $Kr = 10^{-5}$ ms $^{-1}$ and $N_{av} = 1.75 \times 10^{19}$ m $^{-3}$. $\Delta\epsilon = 2$, $e = -40$ pC/m, $W = 10^{-5}$ J/m 2 . Thick line: $\mu^+/\mu^- = 1$; thin line: $\mu^+/\mu^- = 0.1$

When $\mu^+/\mu^- = 0.1$, the large electric field gradient spreads over the layer. The stabilizing torque in the prevailing part of the layer is extremely effective, whereas the destabilizing torque in the right half of the layer is almost negligible. When $\mu^+ = \mu^-$, the gradient is smaller and much less effective. The stabilizing torques are weaker and partially compensated by the destabilizing torques acting in the positive half of the layer. Therefore the enhancement of the threshold does not occur. The deformation appears already at U_T which is comparable with U_f .

4.2.2. $\Delta\epsilon > 0$ and $e_{11} + e_{33} > 0$. The electric field distributions are presented in figure 9 by means of curves calculated for $U = 5.67$ V. This value coincides with the not enhanced upper threshold for the case of $\mu^+ = \mu^-$ (curve 1), whereas it does not induce deformation if $\mu^+/\mu^- = 0.1$ (curve 2). The deformation arises if the electric field $|E(+1/2)|$ reaches a sufficient value at which the surface torque

overcomes the stabilizing effect of the dielectric torque. If $\mu^+/\mu^- = 0.1$, a relatively high voltage is required, i.e. the upper threshold exceeds the U_f value.

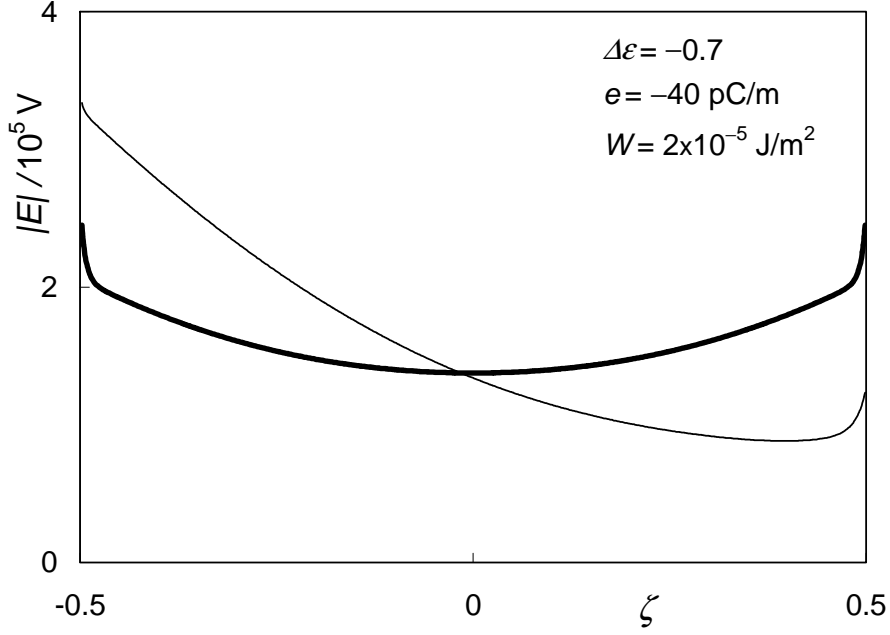


Fig. 8. Electric field strength $|E|$ as a function of the reduced coordinate ζ for $U = 3.19$ V, $Kr = 10^{-5}$ ms $^{-1}$ and $N_{av} = 3.14 \times 10^{18}$ m $^{-3}$. $\Delta\epsilon = -0.7$, $e = -40$ pC/m, $W = 2 \times 10^{-5}$ J/m 2 . Thick line: $\mu^+/\mu^- = 1$; thin line: $\mu^+/\mu^- = 0.1$

When $\mu^+ = \mu^-$, the electric field distribution becomes symmetric. The field value at $|E(+1/2)|$ becomes higher and is sufficient for the deformation already at some lower voltage ($U = 5.67$ V here).

4.3. Occurrence of lower voltage regime, $\Delta\epsilon > 0$ and $e_{11} + e_{33} > 0$

If $\mu^+/\mu^- = 0.1$, we observe appearance of the deformation also in the lower voltage regime (see figure 4). The electric field distributions are shown in figure 9 by means of two curves corresponding to $U = 2.7$ V. For this voltage, the layer is deformed if $\mu^+/\mu^- = 0.1$ (curve 3). On the contrary, for $\mu^+ = \mu^-$ (curve 4), no deformation is observed at this voltage. The deformation is induced by the destabilizing flexoelectric torque, originating due to the electric field gradient in the vicinity of the negative electrode. This gradient becomes lower if μ^+ tends

to μ^- and the resulting torque becomes insufficient. As a consequence, the lower range of voltage disappears (see figure 4).

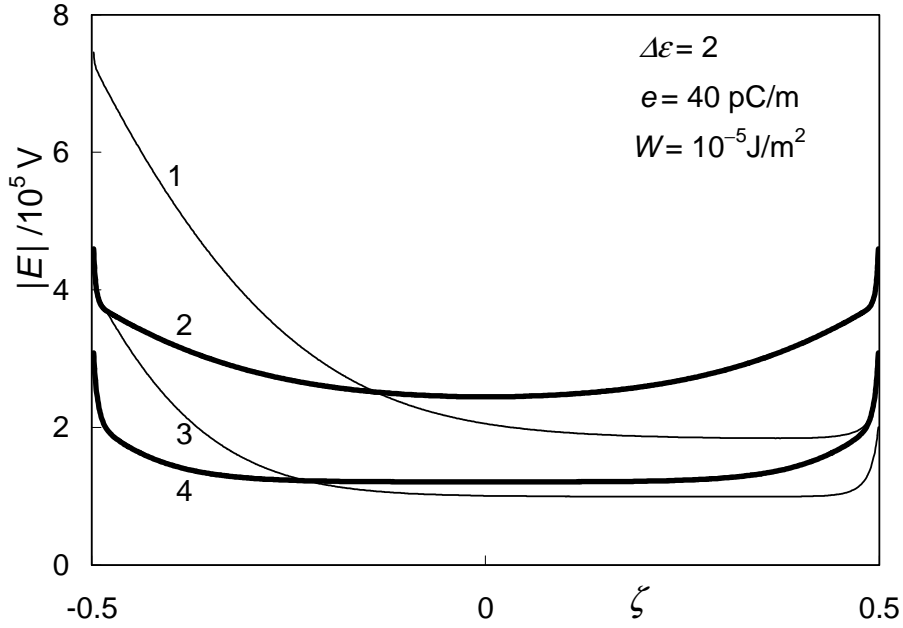


Fig. 9. Electric field strength $|E|$ as a function of the reduced coordinate ζ ; $Kr=10^{-5} \text{ ms}^{-1}$, $\Delta\epsilon=2$, $e=40 \text{ pC/m}$, $W=10^{-5} \text{ J/m}^2$. Average ion concentrations N_{av} (in m^{-3}), voltages U (in volts) and ratios μ^+/μ^- are as follows: 1: $N_{av} = 1.9 \times 10^{19}$, $\mu^+/\mu^- = 0.1$, $U = 5.67$; 2: $N_{av} = 1.21 \times 10^{19}$, $\mu^+/\mu^- = 1$, $U = 5.67$; 3: $N_{av} = 1.73 \times 10^{19}$, $\mu^+/\mu^- = 0.1$, $U = 2.7$; 4: $N_{av} = 1.74 \times 10^{18}$, $\mu^+/\mu^- = 1$, $U = 2.7$

5. CONCLUSIONS

The above considerations show that the peculiar forms of the $U_T(N_{av})$ dependencies shown in figures 1, 2, 3 and 4 have their reason in difference between mobilities of anions and cations. When this reason is removed by increasing of μ^+ , the peculiarities vanish.

The torques which lead to the director field distortions are governed by the electric field within the layer. It is therefore obvious that all the factors which decide on the electric field distribution affect the deformations. The results presented in this paper indicate that the mobilities of ions as well as their ratio

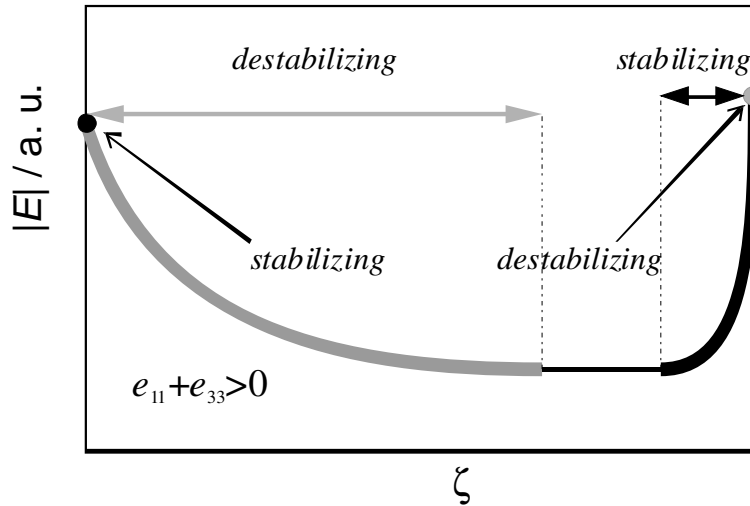


Fig. 10. Schematic relationship between electric field distribution and flexoelectric torques for $e_{11} + e_{33} > 0$. The electric field distributions corresponding to regions of stabilizing and destabilizing torques in the bulk are marked by thick lines, black and grey respectively. Black and grey circles denote the surface fields inducing the surface stabilizing and destabilizing torques. Thin lines denote regions where the flexoelectric torques are negligible. In the case of $e_{11} + e_{33} < 0$, the signs of the torques are opposite

μ^+/μ^- influence the deformation of the flexoelectric nematic layer, since they influence the distributions of the space charge, and in turn determine the $E(z)$ dependence. This statement turns attention to the ion mobilities as a potential source of lack of repeatability of experimental results obtained from different samples.

REFERENCES

- [1] Meyer R.B., Phys. Rev. Lett., **22** (1969) 918.
- [2] Derzhanski A., Petrov A.G., Hinov H.P., Markovski B.L., Bulg. J. Phys., **1** (1974) 165.
- [3] Derzhanski A., Mitov M.D., Compt. Rend. Acad. Bulg. Sci., **28** (1975) 1331.
- [4] Derzhanski A., Petrov A.G., Mitov M.D., J. Phys. (Paris), **39** (1978) 273.
- [5] Barberi R., Barbero G., Gabbasova Z., Zvezdin A., J. Phys. II France, **3** (1993) 147.
- [6] Ponti S., Zihelr P., Ferrero C., Zumer S., Liq. Cryst., **26** (1999) 1171.
- [7] Brown C.V., Mottram N.J., Phys. Rev. E, **68** (2003) 031702.

- [8] Kirkman N.T., Stirner T., Hagston W.E., *Liq. Cryst.*, **30** (2003) 1115.
- [9] Hinov H.P., *Bulg. J. Phys.*, **31** (2004) 55.
- [10] Davidson A.J., Mottram N.J., *Phys. Rev. E*, **65** (2002) 051710.
- [11] Jones J.C., Wood E.L., Bryan-Brown G.P., Hui V.C., *Proc. SID*, **98** (1998) 858.
- [12] Derfel G., Buczkowska M., *Liq. Cryst.*, **32** (2005) 1183.
- [13] Buczkowska M., Derfel G., *Liq. Cryst.*, **32** (2005) 1285.
- [14] Derfel G., Buczkowska M., *Liq. Cryst.*, **34** (2007) 113.
- [15] Naito H., Okuda M., Sugimura A., *Phys. Rev. A*, **44** (1991) R3434.
- [16] Jin M.Y., Kim J.-J., *J. Phys. Condens. Matter*, **13** (2001) 4435.
- [17] Yamashita M., Amemiya Y., *Jpn. J. Appl. Phys.*, **17** (1978) 1513.
- [18] Derfel G., Lipiński A., *Mol. Cryst. Liq. Cryst.*, **55** (1979) 89.
- [19] Briere G., Gaspard F., Herino R., *J. Chim. Phys.*, **68** (1971) 845.
- [20] De Vleeschouwer H., Verschueren A., Bougriona F., Van Asselt R., Alexander E., Vermael S., Neyts K., Pauwels H., *Jpn. J. Appl. Phys.*, **40** (2001) 3272.

ROLA RUCHLIWOŚCI JONÓW W FLEKSOELEKTRYCZNYCH ODKSZTAŁCENIACH PRZEWODZĄCYCH HOMEOTROPOWYCH WARSTW NEMATYCZNYCH

Streszczenie

Przedstawiono wyniki symulacji numerycznych dotyczących zachowania homeotropowej warstwy przewodzącego nematyka posiadającego właściwości fleksoelektryczne i poddanego działaniu zewnętrznego pola elektrycznego. Obliczenia przeprowadzono dla czterech typów materiałów nematycznych scharakteryzowanych przez obydwa znaki anizotropii dielektrycznej i sumy współczynników fleksoelektrycznych. Pokazano, że anomalne zależności napięcia progowego od koncentracji jonów są związane z różnicą ruchliwości jonów dodatnich i ujemnych. Anomalie te zanikają, jeśli ruchliwość kationów staje się bliska ruchliwości anionów. Zaproponowano jakościową interpretację wyników opartą na analizie rozkładu pola elektrycznego w warstwie.